



Adsorption kinetics of zeolite coatings directly crystallized on metal supports for heat pump applications (adsorption kinetics of zeolite coatings)

Lena Schnabel^a, Melkon Tatlier^{b,*}, Ferdinand Schmidt^c, Ayşe Erdem-Şenatalar^b

^a Fraunhofer-Institut für Solare Energiesysteme ISE, Heidenhofstr. 2, D-79110 Freiburg, Germany

^b Department of Chemical Engineering, Istanbul Technical University, Maslak, 34469 Istanbul, Turkey

^c Research Group "Energy and Building Technology", University of Karlsruhe, Kaiserstr. 12, D-76128 Karlsruhe, Bldg. 10.91, Germany

ARTICLE INFO

Article history:

Received 8 April 2009

Accepted 27 February 2010

Available online 6 March 2010

Keywords:

Adsorption

Kinetics

Heat pump

Zeolite

Coating

ABSTRACT

A series of theoretical studies had previously indicated that the utilization of zeolite coatings directly crystallized on metal surfaces might improve the performance of adsorption heat pumps significantly. In this study, for the first time, kinetic measurements were performed to determine the rate of adsorption of zeolite coatings, which is the relevant parameter for increasing the power density of heat pump applications. The zeolite coatings investigated were prepared by using the substrate heating method. A scale-up of the substrate heating system was made in order to be able to grow zeolite coatings on $5 \times 5 \text{ cm}^2$ stainless steel plates, instead of the $1 \times 1 \text{ cm}^2$ plates, conventionally used in synthesis experiments. Two different reactors were constructed in which zeolite A and X coatings, with mass equivalent thicknesses of about $38 \mu\text{m}$ and $230 \mu\text{m}$, respectively, could be obtained. The zeolite X coating, which had a quite open nature, exhibited quite favorable overall adsorption kinetics when compared to a reference sample, a paper-like polymer structure containing zeolite laminated on a metal layer.

© 2010 Elsevier Ltd. All rights reserved.

1. Introduction

Heat management by using adsorption heat pumps may be favorable in many respects. These devices are environmentally friendly, easy to maintain and do not require electrical energy for their operation, except for the control of valves, etc. For these reasons, adsorption heat pumps are being considered as alternatives to classical vapor compression heat pumps. The zeolite–water pair is generally regarded as one of the most suitable adsorbent–adsorbate pairs to be used in these devices.

Research is now mainly focused on increasing the power density and therefore on providing better heat and mass transfer in the adsorber heat exchanger where the adsorbent is placed. For conventional systems, heat transfer resistance mainly originates from the poor contact between the adsorbent, consisting of loose powder or grains, and the heat exchanger. With increasing thickness of the adsorbent layer or packing the low adsorbent thermal conductivity may also lead to significant reductions in the performance of the heat pump.

Different suggestions have been made for improvement, mainly focusing on improving the heat transfer at the boundary and

preparing thin adsorbent layers with high thermal conductivity. The thermal conductivity increased by using a mixture of expanded graphite powders and silica gel powders consolidated by compressive molding [1]. It was also proposed to use zeolite powder filled inside a matrix of expanded graphite [2] or in metal foam [3] in a compact manner. Another approach was to reduce the heat transfer resistance by coating the zeolite powder directly on the heat exchanger surface by gluing [4]. The geometry of the heat exchanger, where high specific area and short thermal distances are necessary, may play an additional role. For example, an adsorbent bed made of finned tubes, which were covered with CaCl_2 in mesoporous silica gel, was prepared [5]. These methods may provide better heat transfer, but this generally occurs at the expense of using additional material (e.g., glue, binder) and making mass transfer the critical issue in the compact adsorbent bed.

The proposal to use zeolite coatings directly crystallized on metal surfaces in adsorption heat pumps may be regarded as a milestone for the provision of a substantial improvement in the performance of these devices. Utilizing zeolite coatings may reduce the resistances to heat transfer in the adsorber, since the thermal contact resistance is eliminated to a great extent, while also providing the opportunity to control resistances to mass transfer [6]. A series of theoretical studies were performed where a mathematical model taking into consideration continuous zeolite coatings synthesized on stainless steel heat exchanger tubes, was used.

* Corresponding author. Tel.: +90 212 2853541; fax: +90 212 2852925.

E-mail address: tatlierm@itu.edu.tr (M. Tatlier).

It was observed that the duration of a single cycle of an adsorption heat pump could be shortened significantly with such an arrangement [6]. The extent of the cycle duration depended on the thickness of the zeolite coating and an optimum thickness value maximizing the useful effect obtained from the heat pump existed in the range 50–150 μm for the cases investigated [7]. The thermodynamic efficiency of the system may be low due to the relatively high metal/zeolite mass ratio. Thus, in case the energy source used to heat the adsorber has significant economical value, relatively thicker coatings might be used. The nature of the coatings is another important factor that will affect the performance of the system. The coating should be well connected but be open in nature. Otherwise, the problems originating from resistances to mass transfer may still, at least partly, prevail.

There are different methods for the preparation of zeolite coatings on various substrates [8–12]. The substrate heating method, in which the metal support is heated directly by the help of a resistance while the reaction mixture is kept cooler in a water bath, allows a better manipulation of zeolite synthesis [13]. In this method, reaction in the mixture may be slowed down significantly while that on the substrate is promoted. Consequently, the phase transformations of the metastable zeolites can be delayed for long periods of time, allowing the growth of relatively thick zeolite coatings. The coatings prepared by this synthesis method exhibited differences in their nature originating from their growth under a thermal gradient. The inhomogeneities in the coating thickness at earlier times of synthesis resulted finally in an accessible sponge-like structure. Zeolite A coatings of about 150 μm mass equivalent thickness could be prepared in previous studies by using the substrate heating method on $1 \times 1 \text{ cm}^2$ stainless steel plates [13]. The equivalent thickness mentioned here is calculated from (mass of zeolite deposited per coated area of substrate)/(density of zeolite). Assuming that the zeolite layer is compact, the density may be represented by that of a zeolite crystal. This value varies between about 1.52 g/cm^3 and 1.99 g/cm^3 for zeolite NaA, when it is dry and saturated, respectively. To obtain similar thicknesses on a larger surface in the substrate heating method is not a straightforward task due to the dependence of synthesis on a higher number of parameters.

In this study, for the first time, kinetic measurements were performed to determine the rate of adsorption of zeolite coatings, which is the relevant parameter for increasing the power density of heat pump applications. Zeolite coatings, directly crystallized on stainless steel plates by using the substrate heating method, were investigated in a test facility, which required the use of coatings of $5 \times 5 \text{ cm}^2$ area. The substrate heating system, therefore, had to be scaled up to prepare coatings of X and A type zeolites on $5 \times 5 \text{ cm}^2$ stainless steel plates, and two different synthesis systems with different geometries were used for this purpose

2. Experimental

2.1. Preparation of zeolite coatings

Zeolite A and X coatings were prepared on stainless steel substrates (AISI 316 grade) by using the substrate heating method. Two reactors with different geometries were utilized to prepare coatings on plates placed either vertically or horizontally in the reaction mixture, as may be seen in Figs. 1 and 2. The devices consisted of polyethylene vessels (1 L), heating resistances (200 W) and stainless steel rods covered with teflon. The resistances inserted into the rods – or cover extensions – were utilized to heat preferentially the side (system 1 shown in Fig. 1) or bottom (system 2 shown in Fig. 2) of the metal rods. Stainless steel plates ($5 \times 5 \times 0.1 \text{ cm}^3$) were placed at the end of the rods either vertically

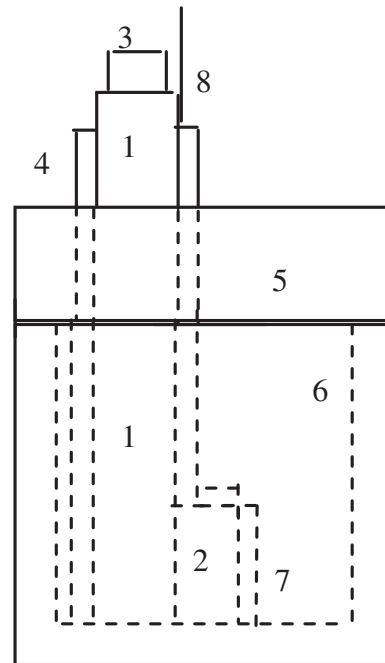


Fig. 1. The substrate heating synthesis system 1 (1: metal cover extension (1), 2: metal cover extension (2), 3: resistance, 4: teflon insulation, 5: vessel cover, 6: synthesis vessel, 7: stainless steel plate, 8: thermocouple).

(system 1) or horizontally (system 2) and were immersed into the reaction mixtures in polyethylene vessels. The temperature was measured by a thermocouple placed on the metal rod near the heating resistance as may be seen from the figures.

The synthesis experiments were carried out in a water bath kept at 25 °C by using a clear solution composition represented by 50 $\text{Na}_2\text{O}:\text{Al}_2\text{O}_3:5 \text{ SiO}_2:1000 \text{ H}_2\text{O}$. Prior to the synthesis of the zeolite coatings, the stainless steel plates were cleaned as reported

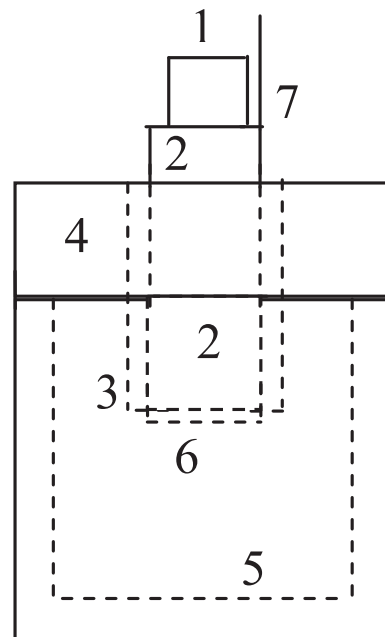


Fig. 2. The substrate heating synthesis system 2 (1: resistance, 2: metal cover extension 3: teflon insulation, 4: vessel cover, 5: synthesis vessel, 6: stainless steel plate, 7: thermocouple).

elsewhere [14]. Granular sodium aluminate (Riedel-de Haen), anhydrous NaOH pellets (Carlo Erba), sodium silicate solution (Merck) and deionized water were used in the synthesis experiments. The coatings prepared were analyzed by X-ray diffraction (Pananalytical X'Pert Pro). XRD was run at an incidence angle of 1° with Cu K α 1 radiation and was applied for phase identification and determination of the purity of the samples.

The reaction mixture composition used in this study is known to yield zeolite A as the initial phase when conventional synthesis is applied and has been utilized widely for the preparation of zeolite A coatings. It should be noted that dilute solutions without organic templates, similar to this mixture, are favorable for the preparation of high-quality zeolite coatings. This is related to the absence of a visible second solid phase (gel) in the mixture as well as to the elimination of the need for calcination. Zeolite A has been reported to form from the composition above after 0.5 h, 1–5 h and 3–9 h at temperatures of 100 °C, 80 °C and 60 °C, respectively [15], by conventional synthesis where phase transformations cannot be delayed for sufficiently long periods. Relatively long synthesis times and higher synthesis temperatures are known to favor the formation of other zeolites, such as X and HS. When the substrate heating method is used, the range of substrate temperature providing zeolite A formation seems to be much more limited for the conditions used in this study (the composition mentioned, and a water bath temperature of 25 °C). Zeolite A coatings could be prepared at a substrate temperature of about 57 °C by using this method for synthesis durations between 3 h and 3 days [13]. However, at a substrate temperature of 72 °C, zeolite A did not form in this system [13]. This was probably related to the significant temperature gradient in the substrate heating system (25–72 °C). Thus, it should not be surprising that a zeolite other than zeolite A may also be formed from this composition as the first phase when the substrate heating method is utilized.

In this study, the zeolite A coating was prepared in system 2 after 3 days of synthesis at a resistance temperature of 60 °C. 3 days of synthesis at a resistance temperature of 220 °C was performed in system 1 to obtain the zeolite X coating. Zeolite A and zeolite X were obtained after 2 days of synthesis, too, in system 2 and system 1, respectively. The surface temperature of the substrate was determined to be around 63 °C and 55 °C when the temperature of the resistance was equal to 220 °C and 60 °C in system 1 and system 2, respectively. The related measurements were performed by using a thermocouple immersed in the solution next to the substrate surface at the beginning of the experiments. The measured values are only approximations of the substrate surface temperature and the actual temperature of the substrate surface might change to some extent as the thickness of the coating increases. The large difference between the resistance temperatures for the two cases investigated originates from the different geometries and heat paths of the systems.

2.2. Measurements of adsorption kinetics

The adsorption kinetics depend on the type of materials (adsorbent, fluid) used, the environmental conditions (starting pressure, temperature, initial loading) as well as the heat and mass transfer properties, mainly determined by the effective heat conductivity and diffusivity inside the adsorbent material and by the contact between the adsorbent and the heat exchanger surface. Since the aim was the optimization of not only the adsorbent structure but also of the combination of adsorbent and metal support, the kinetic measurements were performed on composites, each consisting of an adsorbent and a substrate.

The two different zeolite coatings prepared in this study for use in adsorption heat pumps were characterized in the adsorption

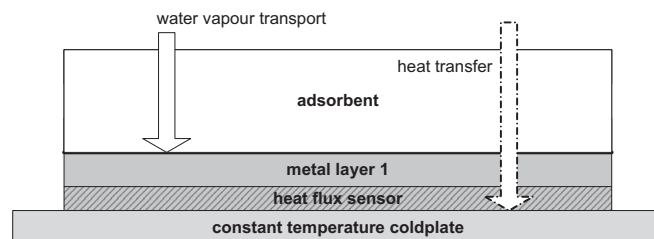


Fig. 3. Scheme of the measured samples.

kinetics test facility in the labs of Fraunhofer ISE. Fig. 3 shows a scheme of the measured sample and its integration into the measurement set up. The coupling between the composite sample and the cold plate was done by a removable heat conductivity paste (Thermigrease TG20031). As can be seen in Fig. 3, between the sample and the cold plate a heat flux sensor was fixed. The cold plate was cooled by water flowing at a high rate at constant temperature, and thus providing an isothermal condition on its surface.

Fig. 4 shows a scheme of the complete kinetic measurement apparatus. The kinetics test facility consisted of two different chambers that might be connected/disconnected by valves. The measuring chamber contained the sample fixed on the cold plate. The other chamber was used as the water vapor reservoir and the dosing chamber. In order to avoid condensation and to realize reproducible ambient conditions, both chambers were located in a large box kept at constant temperature (40 °C). Connecting the dosing chamber with a water vapor source at a given temperature, the equilibrium water vapor pressure at this temperature could be attained. Upon closing the valve between this chamber and the water bath (valve 2), the total mass of water vapor in the chamber could be estimated through an equation of state. For water vapor at low pressures, the calculation was performed by using the ideal gas law.

The pressure was measured inside both chambers by capacitive sensors (MKS Baratron 628), with a range of 1–10,000 Pa with a resolution of 1 Pa. Temperatures were measured with Ni 100 thin film sensors, which have short reaction times and relatively high resolution. For the heat flux measurement a sensor (Captec Enterprise) with an active area of 25 cm² and a sensitivity of 14.4 $\mu\text{V}/(\text{W}/\text{m}^2)$ was used. A computer was used for data logging and controlling the experiment.

The test rig was designed for characterizing adsorbent samples with a mass ranging from 0.1 g to 2 g. For this range of sample mass, starting at 1700 Pa and using the water vapor reservoir with 41.7 L about 0.5 g water can be provided. Due to accuracy reasons, the decrease in pressure should be greater than 100 Pa, but the absolute pressure should not be lower than 5 Pa.

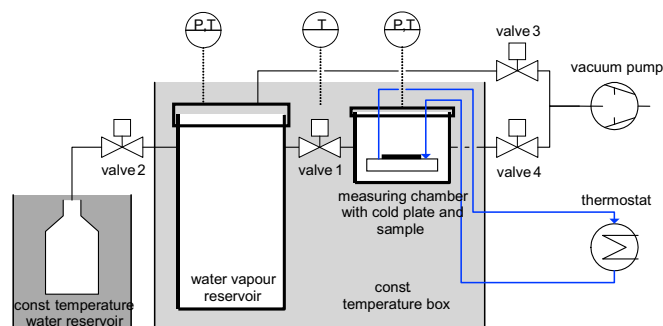


Fig. 4. Scheme of the kinetic measurement test facility.

Table 1
Basic steps of the isothermal measurements.

Step of measurement	Temperature/pressure	Demands
Desorption	95 °C/<1 Pa	Temperature and pressure were constant for 3 h
Cooling	40 °C	Measuring temperature of 40 °C was constant for 1 h in cold plate and thermo box
Preparing the dosing chamber	≈ 1700 Pa	1700 Pa corresponds to 15 °C evaporator temperature
Adsorption	40 °C	Measurement was performed until heat flux signal returned to starting value or there was no more pressure decrease

Before the uptake measurements were performed, the samples were desorbed with similar pre-conditioning, resulting in comparable starting conditions. The basic steps of the isothermal measurements are given in Table 1. Desorption was the first step during which the sample was heated to 95 °C and the measuring chamber was evacuated until pressure, temperature and heat flux signal stayed constant for about 3 h. Using this method for desorption, the initial loading of the sample is not known, but tends to be very close to zero due to the combination of heating and evacuation. More realistic initial conditions can be determined by desorption done by heating and condensation at the given temperature. The initial loading represents a final state of desorption cycle and can be calculated, if equilibrium data are available.

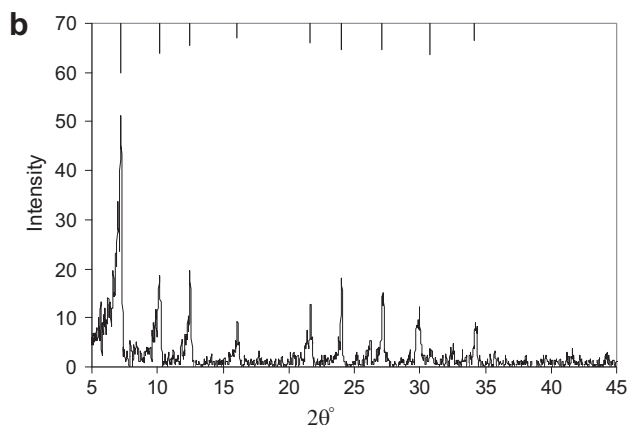
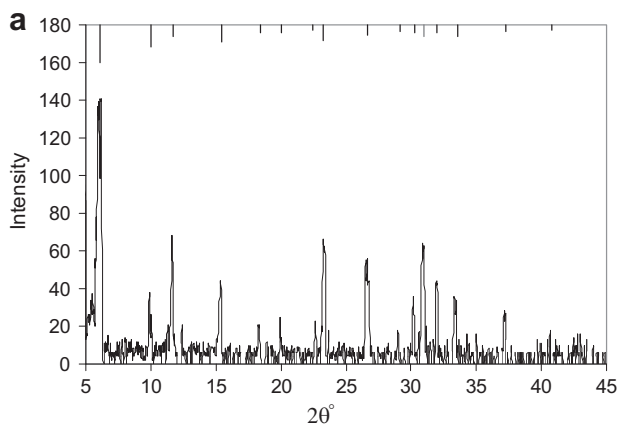


Fig. 5. X-ray diffractograms of a) zeolite X coating prepared in system 1 and b) zeolite A coating prepared in system 2.

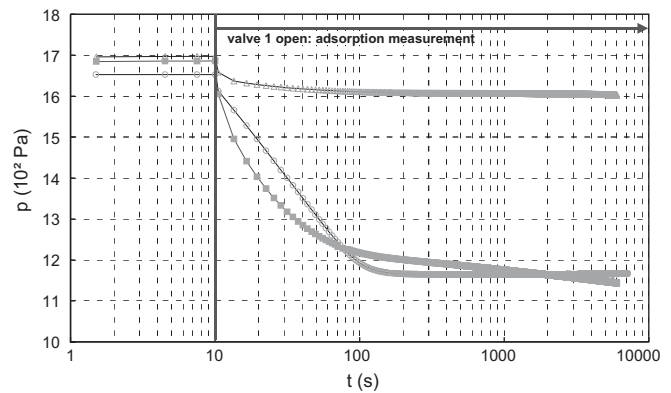


Fig. 6. Variation of measured pressure with time for (■) zeolite X, (Δ) zeolite A and (○) UOP samples.

Compared to the maximum uptake, as done within this work, the initial loading is assumed to be zero. This assumption is reasonable, since from the water isotherm of zeolite X, it may be determined that at this temperature and even at 1 Pa, the water loading in this zeolite is equal to about 0.44% [16].

The second step of pre-conditioning involved the cooling of the sample until the desired temperature was attained and remained constant for 30 min. Simultaneously, the water vapor reservoir was prepared. The water reservoir thermostat was set to the temperature corresponding to the desired vapor pressure. Once the temperature was attained, valve 2 was opened and the water vapor flowed into the reservoir, which had been evacuated before.

After this preparation phase, the sample was dry and the adsorption uptake measurement could be carried out. The measurement started by opening the connection (valve 1) between the measuring chamber and the water vapor reservoir used as the dosing chamber. The sample instantaneously started to adsorb and consequently the measured pressure decreased. Data logging was performed until the pressure and heat flux signal became constant. In a subsequent data processing step the amount of water uptake was calculated by assuming that a decrease in pressure could be attributed directly to an increase in the amount of adsorbed water. The initial amount of water was calculated by using the ideal gas law and the initial pressure, temperature and volume of the dosing chamber. The heat flux signal between the sample and cold plate was also measured and provided an independent signal to determine the adsorption rate.

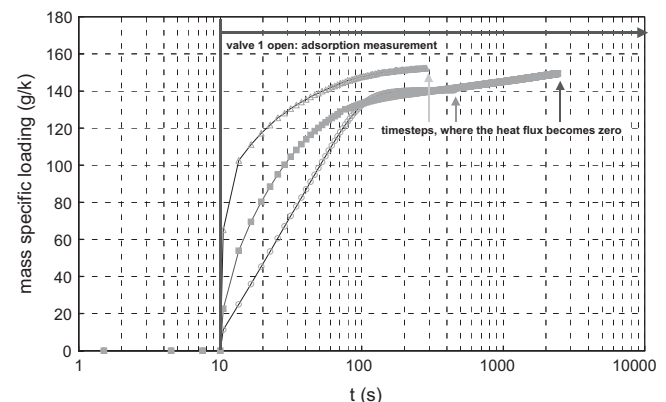


Fig. 7. Variation of water loading with time. Legend as in Fig. 6.

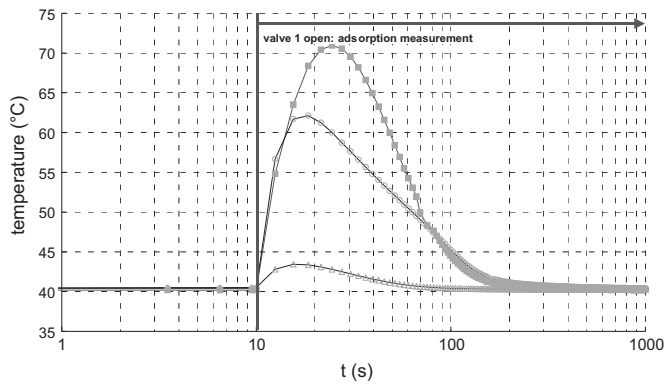


Fig. 8. Variation of temperature measured directly above the sample with time. Legend as in Fig. 6.

3. Results and discussion

The X-ray diffraction patterns of the zeolite X and A coatings prepared by using the substrate heating method may be seen in Fig. 5. Reference patterns for these zeolites are also given in the figure. The zeolite X coating, which was the thicker of the two, had a characteristic sponge-like nature. The zeolite A coating seemed to be more homogeneous and dense. Kinetic measurements were performed for these samples and the result obtained for the zeolite X coating was compared to that obtained for a MOLSIV™ DDZ-70 sample (UOP LLC Company), a paper-like polymer structure containing about 70–80% (by mass) of zeolite laminated on a metal layer [17,18]. The zeolite used here is a steam calcined, rare earth exchanged sodium Y zeolite.

The hydrated masses of the directly crystallized coatings were equal to about 170 mg and 1030 mg for the zeolite A and zeolite X coatings, respectively. The mass deposition on the metal substrates was determined by careful weighing of the samples saturated in a controlled humidity atmosphere provided by an NH_4Cl solution. The mass equivalent thicknesses of these coatings were equal to about 38 μm and 230 μm , respectively. The selected MOLSIV™ DDZ-

70 sample had a thickness of approximately 500 μm and the dry mass of the matrix was about 860 mg. Its hydrated mass was about 1020 mg, therefore, was comparable to that of the directly crystallized zeolite X sample. No direct comparison could be made regarding the kinetics of the zeolite A coating due to the much lower mass of this sample.

The results of the adsorption kinetics experiments are depicted in Figs. 6–10 and Table 2. Fig. 6 shows the variation of the measured pressure with time for the zeolites X, A and UOP samples. The initial pressures were somewhat different due to the variation of the thermostat temperature and varied between 1650 and 1690 Pa. At the tenth second, the valve between measuring and dosing chambers was opened and adsorption started. Different amounts of decrease in the pressure, corresponding to different adsorbent masses, were obtained. The UOP and the zeolite X samples exhibited nearly the same decrease in pressure. The differences in the progression of the curves originated from different heat and mass transfer characteristics.

As described above, the decrease in pressure is directly convertible into water loading. Fig. 7 shows the variation of mass specific loading with time for the three samples, calculated with the hydrated masses given in Table 2. More common and comparable to equilibrium data would be the use of the dry adsorbent mass, but in that case the composite should have been weighed under vacuum conditions and those data were not available. The calculations of the loading curves were stopped at the time-step where the heat flux signal became zero. This allows the evaluation of the loading as depending on sample specific measurement time, which minimizes the error. For the UOP sample, as may be seen from Fig. 7, the steady state and therefore equilibrium was already realized at the time where the heat flux became zero. At the time where the heat flux became zero, an experimentally reproducible decrease in pressure could still be observed for the directly crystallized samples. The reason for this could not be clarified, but the prolonged adsorption might be related to the presence of a small amount of zeolite at the backside of the substrates attached to the cold plate, for these directly crystallized X and A type coatings.

Figs 8 and 9 show the variation of the surface temperature of the sample and the heat flux, measured between the composite sample

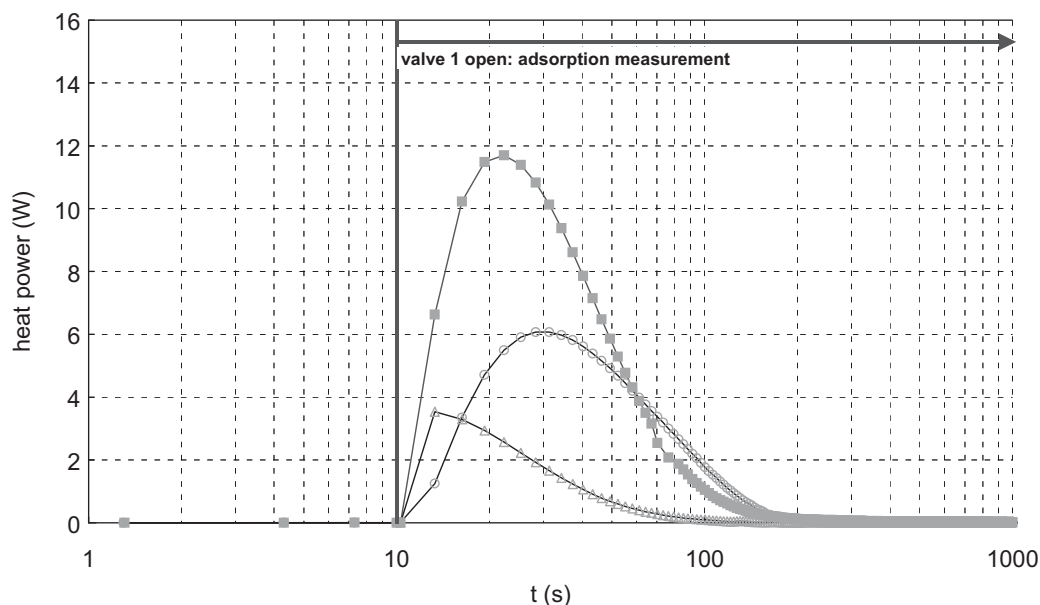


Fig. 9. Variation of heat power measured between the sample and cold plate with time. Legend as in Fig. 6.

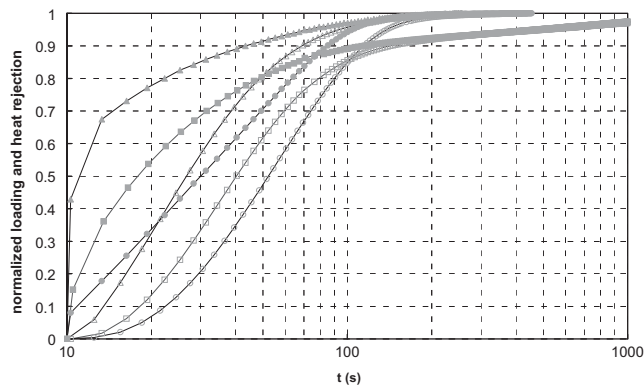


Fig. 10. Variation of normalized heat rejection ((□) zeolite X, (○) UOP, (Δ) zeolite A) and loading ((■) zeolite X, (●) UOP, (▲) zeolite A) with time.

and the cold plate (Fig. 3), with time. The surface temperature was measured by a thin film temperature sensor, which was positioned as close as possible to the adsorbent surface. For the zeolite A and UOP samples this resulted in a plane contact, but due to the filigree structure, the zeolite X sample could be contacted only partly. Due to a heat transfer resistance, the real surface temperature was underestimated for the first few seconds. The comparison of the temperature signals showed maximum surface temperatures of about 62 °C and 70 °C for the UOP and zeolite X samples, respectively, where the UOP sample attained the maximum surface temperature first. The maximum values were reached within 10–20 s, while the cooling down towards the initial temperature of 40 °C took about 200 s. The temperature of the zeolite A sample increased only by about 4 °C. The high surface temperature peak of the zeolite X sample was probably caused by the lower heat conductivity of the adsorbent layer. The high porosity offers a high adsorbent–vapor contact area, but lowers significantly the effective conductivity of the layer.

The heat flux signal in Fig. 9 showed similar trends: the zeolite X sample had the highest peak of about 12 W, followed by the UOP sample with 6 W and zeolite A with 4 W. The maximum was first reached by the thin zeolite A sample, followed by the zeolite X and the UOP samples. The strong increase of the heat flux in the first seconds for the directly crystallized samples could be due to the relatively low heat transfer resistance at the adsorbent–metal contact area.

Fig. 10 shows the variation of the normalized heat rejection and loading with time. Here, the actual measured value was divided by the final loading or the amount of released heat. Due to the thermal resistances, the heat rejection was always delayed compared to the normalized loading. It may be observed from Fig. 10 and Table 2

Table 2

Results of the kinetic measurements made for zeolite A and X coatings and their comparison with the UOP sample.

Identification	Zeolite A	Zeolite X	UOP
Adsorbent mass at ambient conditions (mg)	170	1030	1020
Equivalent thickness (μm)	38	230	500
Starting pressure (Pa)	1696	1684	1653
Realized pressure decrease (Pa)	88	524	489
Adsorbed water (mmol)	1.4	8.5	8.0
Heat detected (J)	90	564	416
Heat detected per mol (kJ/mol)	63	66	52
Maximum uptake (mg/g)	152	149	140
t_{90} of heat rejection (s)	63	138	111
t_{90} of loading (s)	39	108	78
t_{80} of heat rejection (s)	45	75	84
t_{80} of loading (s)	18	42	57

that the UOP sample completed 80% and 90% of its water vapor uptake after about 57 s and 78 s, respectively. These durations were equal to about 18 s and 39 s for the zeolite A coating and to about 42 s and 108 s for the zeolite X coating, respectively. The directly crystallized zeolite X sample was generally faster than the UOP sample in completing the water vapor uptake. Due to the prolonged adsorption, the 90% threshold was reached later for the zeolite X sample. The same tendency could be seen for the normalized heat rejection. All the time values are given in Table 2.

The cooling power of an adsorption heat pump cycle may be defined as

$$P = Q_e/t \quad (1)$$

where t represents the duration of a single cycle. Q_e represents the cooling effect that may be obtained from the evaporator in a single cycle and it may be defined as follows:

$$Q_e = \Delta W m_{ads} L - C_{pw} m_{ads} \Delta W (T_c - T_e) \quad (2)$$

ΔW represents the amount of water circulating in the system. m_{ads} , C_{pw} and L denote the amount of adsorbent in the adsorber, the specific heat capacity of water and the latent heat of vaporization of water, respectively. T_c and T_e correspond to the temperatures of the condenser and evaporator.

The cooling power of an adsorption heat pump, utilizing the zeolite X and UOP samples investigated in this study, was estimated by taking into consideration the durations required to adsorb different amounts of water. The aim was to compare the performances of these two samples that had similar mass values. The length of the desorption period was assumed to be equal to that of the adsorption period. Thus, the cooling power was determined by dividing the cooling effect (Q_e) by $2 \times t_{ads}$ where t_{ads} denotes the time when the samples completed the adsorption of 20%, 40%, 60%, 80% or 90% of their maximum loading. A difference of 15 °C was assumed for $T_c - T_e$ and the power was estimated per mass of adsorbent.

The variation of power with respect to the normalized loading may be seen in Fig. 11 for the zeolite X and UOP samples. It may be observed that when the samples completed 20% of their uptakes, the power provided by zeolite X was about 6 fold higher than that of the UOP sample. The difference between the power values decreased for the higher normalized loadings and after 80% of the uptake was completed, the power was almost equal for both samples. Since the adsorption capacities of the two samples were comparable, this was understandable. The significantly better performance of zeolite X especially at the early periods of adsorption indicated its superior overall adsorption kinetics compared to

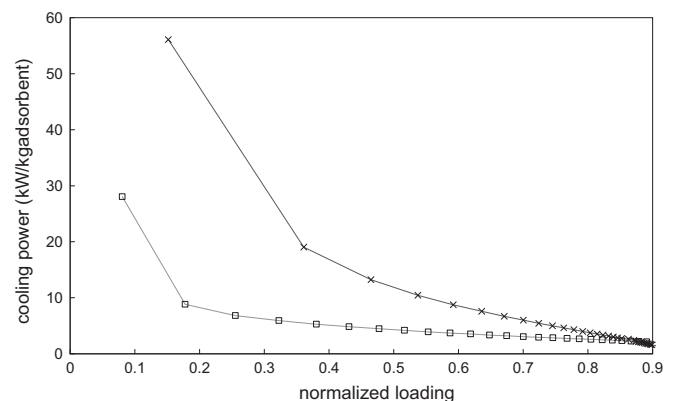


Fig. 11. Variation of cooling power with normalized loading for (x) zeolite X and (□) UOP samples.

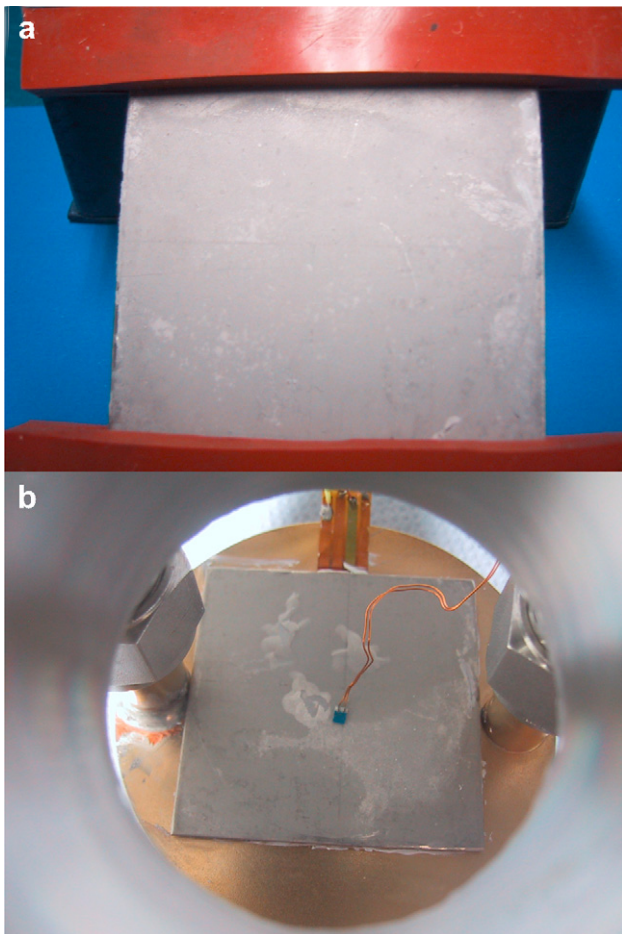


Fig. 12. Pictures of the zeolite A coating (a) before and (b) after the kinetic measurement.

the UOP sample. The zeolite X coating prepared by using the substrate heating synthesis method seemed to possess favorable properties for adsorption heat pumps. The performances of the samples should also be checked under typical operating conditions of a heat pump for further evaluation of the actual power that they may provide.

The coatings prepared by the substrate heating method were shown to exhibit differences in their nature originating from their growth under a thermal gradient [13]. The inhomogeneities in the coating thickness at earlier times of synthesis resulted finally in an accessible sponge-like structure. The superior performance of the zeolite X coating in this study might be considered to originate from the open nature of this coating, related to the presence of non-zeolite macrovoids, which may ease the diffusion of water, as well as to the low heat transfer resistance on the adsorbent–metal contact area.

For the performance of a heat pump system and its economic lifetime, the properties and durability of the adsorbent layer are of utmost importance. The coatings may undergo permanent change upon exposure to temperature and mechanical stressing induced by thermal expansion. Additionally, the heat pump unit should withstand the mechanical stressing during transportation and assembling. Thus, a lifetime test of the adsorbent layer with the metal of the heat exchanger should be done to show special damages of the layering of the connection between the adsorbent and metal.

The zeolite A and X coatings prepared in this study both showed good mechanical properties during preparation. Some small part of the zeolite A sample was displaced during the measurement, as can be seen in Fig. 12. This might have been a result of insufficient connection between metal and adsorbent. The zeolite X sample exhibited a crack on the surface of about 2 cm length. In some parts of the region where the crack was observed, the contact between the adsorbent and substrate was weakened. However, during the measurement, the coating remained intact and no significant displacement occurred. Fig. 13 shows pictures of the zeolite X coating as taken after the kinetic measurement. It may be seen that

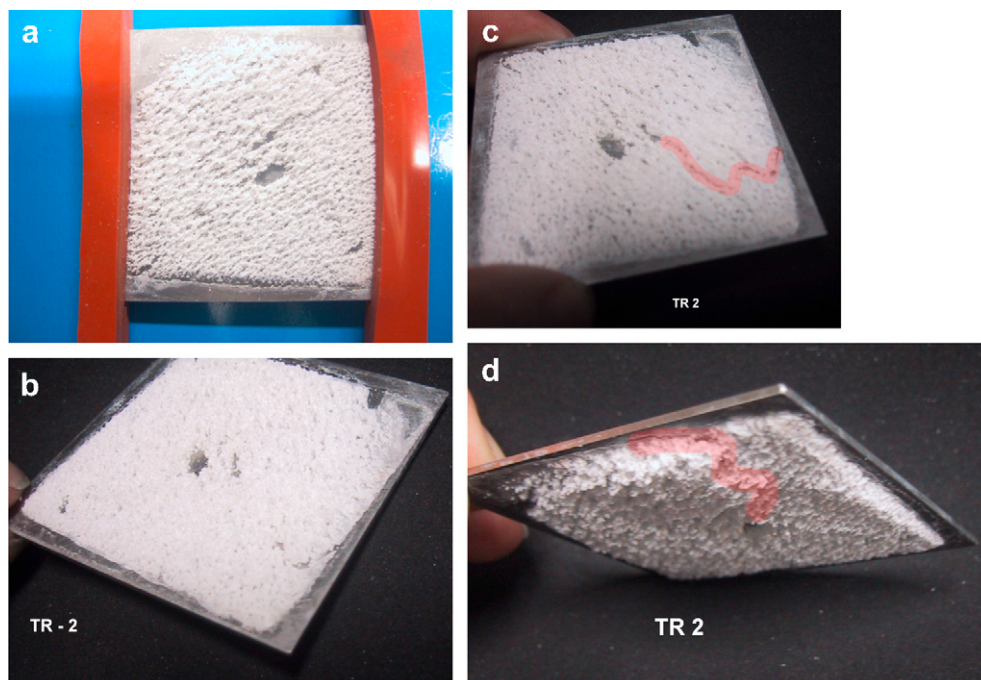


Fig. 13. Pictures of the zeolite X coating (a) before and (b–d) after the kinetic measurement.

the coating kept its integrity even when it was held upside down (Fig. 13d). The properties of the substrate heating system and the experimental conditions, such as the substrate temperature and the composition of the initial reaction mixture affect the stabilities of the coatings to some extent. The stability issue will be investigated systematically and in more detail in a future study. The effects of using different experimental conditions as well as pre/post-synthesis treatments, such as increasing the substrate roughness, will be investigated in this context.

4. Conclusions

The zeolite X coating prepared by using the substrate heating method exhibited promising adsorption kinetics properties for heat transformation applications. This directly crystallized sample exhibited a better performance at least up to 85% of final loading and heat rejection, compared to the reference sample consisting of a polymer–zeolite structure glued on metal support. According to the experimental results obtained, the heat transfer resistance between the crystal and the metal layer of the zeolite A and X coatings seemed to be lower than that of the reference sample, whereas the open pore structure of the zeolite X sample reduced the effective conductivity of the layer. When the overall performances were taken into consideration, it was estimated that the power of an adsorption heat pump utilizing the zeolite 13X coating prepared in this study could be significantly higher than that of a similar system utilizing the reference sample, especially at the relatively low amounts of the normalized loading. This was due to the open nature of this coating, related to the presence of non-zeolite macrovoids, which may ease the diffusion, as well as to the low heat transfer resistance on the adsorbent–metal contact area.

Investigating the use of different reactor geometries as well as other reaction mixture compositions in the preparation of zeolite coatings may be useful to provide materials that have even more favorable properties for heat pump applications and that are more stable.

Acknowledgements

This work was carried out as part of a project (No 107M076) sponsored by The Scientific & Technological Research Council of Turkey (TÜBİTAK) and was supported by the Scholarship Programme of the German Federal Environmental Foundation (DBU). Additionally we gratefully acknowledge Steve Dunne at the UOP LLC Company for providing the adsorbent material.

References

- [1] T.-H. Eun, H.K. Song, J.H. Han, K.-H. Lee, J.-N. Kim, Enhancement of heat and mass transfer in silica-expanded graphite composite blocks for adsorption heat pumps: part I. Characterization of the composite blocks. *International Journal of Refrigeration* 23 (2000) 64–73.

- [2] J.J. Guilleminot, J.B. Chalfen, F. Poyelle, Transfers de masse et de chaleur dans les Composites Adsorbents Consolides. Influence sur les Performances d'une Pompe à Chaleur à Adsorption Solide, in: , Proceedings of 19th International Conference of Refrigeration, vol. IV, 1995, pp. 261–268 The Hague, Netherlands.
- [3] J.J. Guilleminot, A. Choisier, J.B. Chalfen, S. Nicolas, J.L. Reymoney, Heat transfer intensification in fixed-bed adsorbents. *Heat Recovery Systems & CHP* 13 (1993) 297–300.
- [4] J.J. Guilleminot, J.B. Chalfen, A. Choisier, Heat and mass transfer, characteristics of composites for adsorption heat pumps, in: , Proceedings of International Adsorption Heat Pump Conference, vol. 31. AES, New Orleans, 1994, pp. 401–406.
- [5] F. Freni, S. Russo, M. Vasta, Y.I. Tokarev, Y.I. Aristov, G. Restuccia, An advanced solid sorption chiller using SWS-1L. *Applied Thermal Engineering* 27 (2007) 2200–2204.
- [6] M. Tatlier, B. Tantekin-Ersolmaz, A. Erdem-Şenatalar, A novel approach to enhance heat and mass transfer in adsorption heat pumps using the zeolite–water pair. *Microporous and Mesoporous Materials* 27 (1999) 1–10.
- [7] M. Tatlier, A. Erdem-Şenatalar, Effects of metal mass on the performance of adsorption heat pumps utilizing zeolite 4A coatings synthesized on heat exchanger tubes. *International Journal of Refrigeration* 23 (2000) 260–268.
- [8] S. Yamazaki, K. Tsutsumi, Synthesis of an A-type zeolite membrane on silicon oxide film–silicon, quartz plate and quartz fiber filter. *Microporous Materials* 4 (1995) 205–212.
- [9] L. Bonaccorsi, A. Freni, E. Proverbio, G. Restuccia, F. Russo, Zeolite coated copper foams for heat pumping applications. *Microporous and Mesoporous Materials* 91 (2006) 7–14.
- [10] F. Scheffler, R. Herrmann, W. Schwieger, M. Scheffler, Preparation and properties of an electrically heatable aluminium foam/zeolite composite. *Microporous and Mesoporous Materials* 67 (2004) 53–59.
- [11] D.E. Beving, C.R. O'Neill, Y. Yan, Hydrophilic and antimicrobial low-silica–zeolite LTA and high-silica–zeolite MFI hybrid coatings on aluminum alloys. *Microporous and Mesoporous Materials* 108 (2008) 77–85.
- [12] W. Schwieger, R. Herrmann, T. Selvam, R. Marthala, F. Scheffler, F. Schmidt, W. Mittelbach, H.-M. Henning, J. Bauer, Method for Production of a Substrate Coated with a Zeolite Layer, International Patent, WO2006048211006, 2006.
- [13] A. Erdem-Şenatalar, M. Tatlier, M. Ürgen, Preparation of zeolite coatings by direct heating of the substrates. *Microporous and Mesoporous Materials* 32 (1999) 331–343.
- [14] J.C. Jansen, D. Kaschiew, A. Erdem-Şenatalar, Preparation of coatings of molecular sieve crystals for catalysis and separation. *Studies in Surface Science and Catalysis* 85 (1994) 215–250.
- [15] P. Wenging, S. Ueda, M. Koizumi, The synthesis of zeolite NaA from homogeneous solutions and studies of its properties, in: *New Developments in Zeolite Science and Technology*. Elsevier, Tokyo, 1986, pp. 177–184.
- [16] Y. Wang, M.D. LeVan, Adsorption equilibrium of carbon dioxide and water vapor on zeolites 5A and 13X and silica gel: pure components. *Journal of Chemical & Engineering Data* 54 (2009) 2839–2844.
- [17] M.-W. Tang, S.R. Dunne, P.K. Coughlin, Adsorbent Sheet, Process of Preparing and Desiccant Process for Using the Sheet, International Patent, WO 02/45847 A2, 2002.
- [18] L. Schnabel, H.-M. Henning, Experimental and simulation study on the kinetics of water vapour adsorption on different kinds of adsorptive material matrices, in: *Proceedings of International Sorption Heat Pump Conference (ISHPC)*, Denver, USA, 2005, pp. 1–8.

Nomenclature

- C_{pw} : specific heat capacity of water (J/kg K)
 L : latent heat of vaporization of water (J/kg)
 m_{ads} : adsorbent mass (kg adsorbent)
 P : power (W)
 Q_e : useful heat obtained from the evaporator in a single cycle (J)
 t : duration of a single cycle (s)
 T_c : condenser temperature (K)
 T_e : evaporator temperature (K)
 ΔW : amount of water circulating in the system (kg/kg adsorbent)